

UC Irvine

ICTS Publications

Title

Activation of PKC α and PI3K Kinases in Hypertrophic and Nodular Port Wine Stain Lesions.

Permalink

<https://escholarship.org/uc/item/65p7w38f>

Journal

The American Journal of dermatopathology, 39(10)

ISSN

1533-0311

Authors

Yin, Rong
Gao, Lin
Tan, Wenbin
et al.

Publication Date

2017-10-01

Copyright Information

This work is made available under the terms of a Creative Commons Attribution License, available at <https://creativecommons.org/licenses/by/4.0/>

Peer reviewed

Activation of PKC α and PI3K Kinases in Hypertrophic and Nodular Port Wine Stain Lesions

Rong Yin, MD,*† Lin Gao, MD, PhD,* Wenbin Tan, MD, PhD,‡ Wei Guo, MD,*
Tao Zhao, MD,* Jhon Stuart Nelson, MD, PhD,‡§ and Gang Wang, MD, PhD*

Abstract: Port wine stain (PWS) is a congenital, progressive vascular malformation. Many patients with PWS develop hypertrophy and discrete nodularity during their adult life, but the mechanism(s) remain incompletely understood. In this study, we attempted to investigate activation status of PKC α , PI3K, PDK1 and PLC- γ and protein levels of PP2A and DAG to explore their potential roles in the formation of hypertrophic and nodular PWS lesions. We found phosphorylated levels of PKC α , PI3K, PDK1, and PLC- γ and protein levels of PP2A and DAG showed moderate increases in the endothelial cells of hypertrophic PWS as compared to the adjacent normal skin. These increases extended throughout the entire stroma of blood vessels in PWS nodules. Many proliferating cells, such as fibroblasts, also showed strong activation of PKC α , PI3K, PDK1 and PLC- γ and upregulations of PP2A and DAG in nodular PWS lesions. Our data showed that there is aberrant activation of PKC α , PI3K, PDK1 and PLC- γ and upregulation of PP2A and DAG mainly in endothelial cells in hypertrophic PWS areas, but presenting in the entire vasculatures and surrounding fibroblasts in PWS nodules. Our data suggest that both PKC α and PI3K signaling pathways contribute to the development of hypertrophy and nodularity in adult PWS.

Key Words: port wine stain, PI3K, PKC α , PLC- γ , PDK1, vascular malformation

(*Am J Dermatopathol* 2017;39:747–752)

INTRODUCTION

Port wine stain (PWS) is a congenital, progressive vascular malformation of human skin involving the superficial

From the *Department of Dermatology, Xijing Hospital, Fourth Military Medical University, Xi'an, China; †Departments of Dermatology, The Second Clinical Medical College, Shanxi Medical University, Taiyuan, China; ‡Department of Surgery, Beckman Laser Institute and Medical Clinic, University of California, Irvine, CA; and §Department of Biomedical Engineering, University of California, Irvine, CA.

Supported by National Natural Scientific Foundation of China (81301355 to LG, 81430073 and 81220108016 to GW), and NIH AR063766 to WT.

R. Yin and L. Gao contributed equally to this work.

The authors have no conflict of interest to declare.

Reprints: Gang Wang, MD, PhD, Department of Dermatology, Xijing Hospital, Fourth Military Medical University, Xi'an 710032, China (e-mail: xjwgang@fmmu.edu.cn).

Copyright © 2016 The Author(s). Published by Wolters Kluwer Health, Inc. This is an open-access article distributed under the terms of the Creative Commons Attribution-Non Commercial-No Derivatives License 4.0 (CCBY-NC-ND), where it is permissible to download and share the work provided it is properly cited. The work cannot be changed in any way or used commercially without permission from the journal.

vascular plexus that occurs in estimated 3–5 children per 1,000 live births.^{1–3} Because most malformations occur on the face, PWS is a clinically significant problem in the majority of patients. Personality development is adversely influenced in virtually all patients by the negative reaction of others to a “marked” person. Detailed studies have documented lower self-esteem in such patients and problems with interpersonal relationships.^{4–6}

In childhood, PWS are flat red macules, but lesions tend to darken progressively to purple and, by middle age, often become raised as a result of the development of vascular nodules.^{7,8} The late-stage cobblestoning appearance of PWS subjects is comprised by not only pronounced vascular ectasia with proliferation of thin and/or thick-walled vessels and their stroma, but also numerous epithelial, neural and mesenchymal hamartomatous abnormalities.⁹ Despite these histologic observations, the specific mechanisms involved in PWS nodular formation remains unclear. Our previous data have shown a sequential activation profile of various kinases during different stages of PWS.¹⁰ In one nodular PWS subject, we found that phosphatidylinositol 3-kinases (PI3K)/protein kinase B (AKT) and phosphoinositide phospholipase C γ subunit (PLC- γ) were activated in both hypertrophic areas and nodules within the lesion.¹⁰ These observations led us to hypothesize that the PI3K pathway may play an important role in nodular formation. In this study, we attempt to further investigate the phosphorylation levels of various kinases involved in the PI3K pathway, including 3-phosphoinositide-dependent protein kinase-1 (PDK1), protein kinase C alpha (PKC α), protein phosphatase 2 α (PP2A), PI3K, 1,2-Diacylglycerol (DAG) and PLC- γ , in hypertrophic and nodular PWS lesions.

MATERIALS AND METHODS

Patients and Tissue Samples

The study was approved by the Investigational Review Board at the Xijing Hospital, Xi'an, China. A total of 21 PWS biopsy samples, including 8 hypertrophic, 8 nodular PWS specimens, and 5 specimens from adjacent normal skin 0.5–1 cm away from PWS lesions, were obtained from 13 subjects and deidentified for this study. Two normal adult skin samples were retrieved from the skin biopsy tissue bank from our department to serve as normal controls. We categorize PWS nodules into 2 types based on their histopathological characterizations. Type 1 is mainly composed of large ectatic, thick

TABLE 1. Clinical Description of Adult PWS Subjects and Types of Biopsied Samples

Patient Number	Gender	Diagnosis	Treatment History	Other Vascular Malformations	Type of Biopsied Samples
1	M	PWS face, hypertrophic	None	No	Hypertrophic
2	M	PWS face, hypertrophic	PDL	No	Hypertrophic
3	M	PWS, upper-middle back, nodular	None	No	Nodular type 2
4	M	PWS, chest, nodular	None	No	Nodular type 2
5	M	PWS face, nodular	None	No	Adjacent skin, hypertrophic, Nodular type 1, Nodular type 2
6	M	PWS face, hypertrophic	PDL	No	Hypertrophic, Adjacent skin, Nodular type 2
7	M	PWS face, nodular	None	No	Nodular type 2
8	M	PWS face, nodular	PDL	No	Nodular type 1, Adjacent skin, Nodular type 1, Nodular type 2
9	F	PWS face, nodular	PDL	No	Nodular type 1, Nodular type 2
10	M	PWS face, hypertrophic	None	No	Hypertrophic
11	F	PWS face, hypertrophic	None	No	Hypertrophic, Adjacent skin, Hypertrophic
12	F	PWS neck, hypertrophic	PDL	No	Hypertrophic
13	F	PWS face, hypertrophic	None	No	Hypertrophic, Adjacent skin, Normal skin
14	F	Normal face	None	No	Normal skin
15	M	Normal face	None	No	Normal skin

or thin-walled blood vessels. Type 2 has vascular lobules as the vascular proliferative sites. It is composed of massive capillaries and venule-like vasculatures with both ectatic and/or nonectatic blood vessels. Nodular patients may present either one or both types of nodules within their lesions. The clinical history of PWS subjects and list of biopsy samples are showed in Table 1.

Histology

Skin specimens were fixed in Bouin's solution overnight. Then, they were dehydrated, cleaned, and embedded in paraffin and sectioned to 5 μ m thick. The sections were stained with hematoxylin and eosin (H&E) and photographed under an optical microscope.

Immunohistochemistry

Routine immunohistochemistry procedures were used as follows. Briefly, the fresh biopsy tissue was fixed in 10% buffered formalin (Fisher Scientific, Pittsburgh, PA) and processed for permanent paraffin embedding on an ASP 300 tissue processor (Leica Microsystems, Bannockburn, IL). Approximately 6- μ m-thick paraffin sections were cut and collected. Antigen retrieval was performed in 10 mM sodium citrate buffer (pH 6.0) at 97 °C for 4–5.5 hours. Sections were then incubated in a humidified chamber overnight at 4 °C with

the following primary antibodies: anti-p-PI3K (Santa Cruz Biotech., Santa Cruz, CA), anti-p-PKC α (Abcam, Cambridge, MA), anti-p-PLC- γ (Santa Cruz Biotech), anti-p-PDPK1 (Santa Cruz Biotech), anti-PP2A (Abcam), and anti-DAG (Abcam). Biotinylated anti-mouse and anti-rabbit secondary antibodies were incubated with the sections for 2 hours at room temperature after the primary antibodies' reaction. An indirect biotin avidin diaminobenzidine (DAB) system (Dako, Glostrup, Denmark) was used for detection. The cellular immunoreactivity score was evaluated using a system previously reported by Populo et al.¹¹ Briefly, four scales were used to evaluate the immunoreactive (IR) intensity scores: 0 (no staining), 1+ (weak), 2+ (intermediate), and 3+ (strong staining). Two scales were used to assess the percentage scores of IR cells: 1 (\leq 30%) and 2 ($>$ 30%). The final immunoreactivity scores of each antibody were estimated by multiplying the IR intensity and percentage scores, which were categorized as follows: 0 (negative), 1 (low), moderate (2, 3, and 4), and 6 (high).¹¹ The summary of antibodies we used and their resources were listed in Table 2.

RESULTS

Typical pathological features of vascular anomalies were observed in a series of biopsies from adjacent normal skin to

TABLE 2. Summary of the Antibodies Used in This Study

Antibody	Clone/Catalog	Epitope	Species	Dilution	Source
p-PI3K	polyclonal	p85 α -Tyr 467	Rabbit	1:100	Santa Cruz Biotech., Santa Cruz, CA
p-PKC α	monoclonal	Phospho S657 + Y658	Rabbit	1:100	Abcam, Cambridge, MA
p-PLC- γ	polyclonal	Tyr 783	Goat	1:100	Santa Cruz Biotech., Santa Cruz, CA
p-PDPK1	polyclonal	Ser 241	Rabbit	1:100	Santa Cruz Biotech., Santa Cruz, CA
PP2A	monoclonal	PP2A α + β Y119	Rabbit	1:500	Abcam, Cambridge, MA
DAG	polyclonal	DAG1	Goat	1:100	Abcam, Cambridge, MA

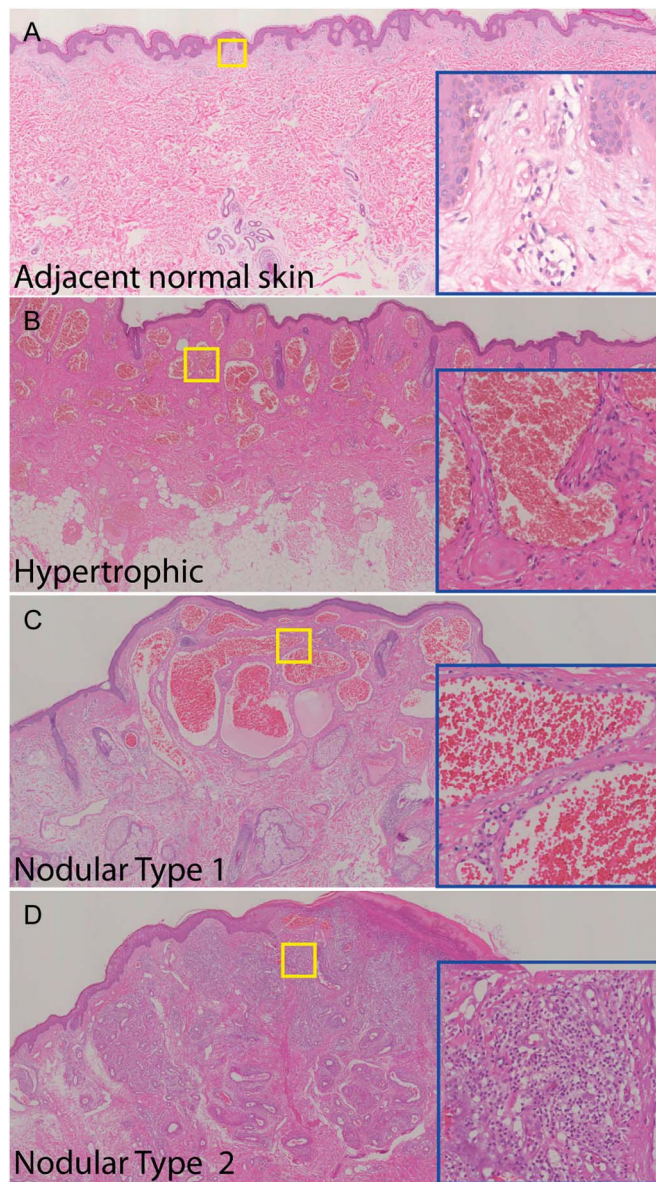


FIGURE 1. Histopathology of vascular anomalies in adjacent normal skin (A), hypertrophic area (B), and 2 types of nodules within the lesions from a PWS nodular subject (C, D) (#5). H&E staining. The blue insets are higher magnifications of the yellow boxed areas.

hypertrophic areas to nodules within the lesions obtained from one facial nodular PWS subject (Fig. 1, Table 1, subject #5). Some capillaries and venule-like vasculatures in the reticular dermis in the normal adjacent skin showed mild enlargement (Fig. 1A), indicating the presence of some initial pathological changes. In the areas of PWS hypertrophy, there were numerous ectatic, thick or thin-walled vasculatures engorged with blood throughout the entire dermis (Fig. 1B). The nodules arising from PWS hypertrophied regions usually had one or both of the following types of structures: type 1 was mainly composed of large ectatic, thick or thin-walled blood vessels; and type 2 contained vascular lobules that appeared as

proliferating vascular sites that were composed of massive capillaries and venule-like vasculatures, with both ectatic or nonectatic blood vessels. The proliferation of pericytes and fibroblasts was present in both cases, but more evident in type 2 (Fig. 1D) as compared to type 1 nodules (Fig. 1C).

In the normal skin adjacent to PWS, endothelial cells (ECs) in those nondilated blood vessels showed very mild IR signals for the p-PI3K, p-PKC α , p-PLC- γ , and p-PDPK1. Some scattered pericytes and fibroblasts with moderate IR signal for these antibodies were also observed. The early dilated blood vessels showed an increase in activation of these kinases (Figs. 2, 3). In hypertrophic PWS, ECs and a small portion of pericytes showed moderate to strong activation of PI3K, PKC α , PLC- γ , and PDPK1. The scattered IR-positive fibroblasts could also be observed. Strong activation of PI3K, PKC α , PLC- γ , and PDPK1 was shown in all ECs and the majority of replicated pericytes and fibroblasts that surrounded PWS blood vessels in the nodules (Figs. 2, 3). There were scattered individual ECs, pericytes, and fibroblasts with very mild to moderate activation of PI3K, PKC α , PLC- γ , and PDPK1 in normal skin. The relative IR intensity scores of p-PI3K, p-PKC α , p-PLC- γ , and p-PDPK1 showed a progressive increase from normal skin to hypertrophic to nodular PWS, which were positively correlated with PWS pathological progression (Fig. 4).

In normal skin adjacent to PWS lesions, there was no obvious IR signal observed. A mild IR signal for PP2A could be mainly observed in some scattered pericytes and fibroblasts (Fig. 3). A moderate expression of DAG was observed in approximately two-thirds of ECs and a few scattered pericytes in hypertrophic lesional areas. In nodules, all ECs and a few scattered pericytes and fibroblasts had a moderate-to-strong IR signal for DAG. PP2A showed a moderate expression level in all ECs and a few scattered pericytes in hypertrophic lesional areas, but it had a very strong IR signal throughout the entire thickened blood vessels, including ECs, replicated pericytes and fibroblasts, in nodules (Fig. 3). The increase in relative IR intensity scores of DAG and PP2A correlated with the pathological progression of PWS lesions (Fig. 4).

DISCUSSION

There have been 2 long-standing hypotheses regarding the pathogenesis of PWS birthmarks. One is a lack of nerve innervation to blood vessels contributing to development of PWS; the other is genetic mutations causing PWS, which is now favored by many researchers. Recent studies have suggested that sporadic somatic mutations of guanine nucleotide-binding protein, G alpha subunit q (*Gnaq*) (R183Q) and phosphatidylinositol 3-kinase catalytic, alpha polypeptide (*Pi3kca*) are linked to the vascular phenotypes of PWS.¹²⁻¹⁴ Shirley et al¹³ first discovered a low-frequency somatic mutation in the *Gnaq* gene (c.548 G \rightarrow A, p.R183Q) present in PWS lesions. We and Cuoto et al further identified that *Gnaq* (R183Q) is primarily present in blood vessels (60%)^{15,16} and/or in connective tissue (30%)¹⁶ and hair follicle/glands (20%)¹⁶ in PWS lesions. These data suggest that pluripotent cells with *Gnaq* (R183Q) may give rise to multilineages in PWS.¹⁶ Another

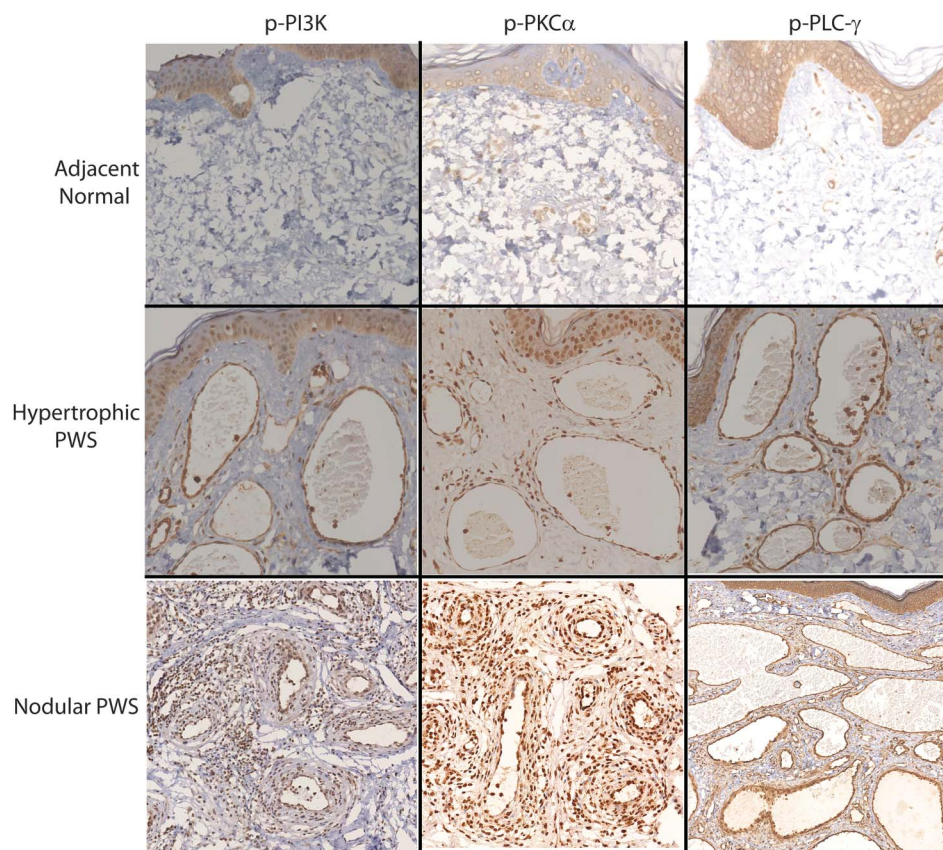


FIGURE 2. Activation of PI3K, PKC α , and PLC- γ in the blood vessels from different types of PWS lesions.

important candidate gene is *Pi3kca* where a mutation (p.G1049N) has been identified in PWS nodular lesions.¹² Other somatic mutations, such as p.C420R, p.E542K, p.E545K, p.H1047R and p.H1047L, have been found in lymphatic and vascular malformation disorders.¹⁴ These findings suggest that *Pi3kca* alone or together with other genetic alterations, such as *Gnaq* mutations or environmental factors, contribute to the development of PWS. The mutation status of the *Pi3kca* and *Gnaq* genes in these PWS subjects studied here is unknown, which will be a subject of future study.

Finley proposed in 1984 that the cobblestoning appearance of the skin surface, thickening, and discrete nodular growths that develop during the adult life of PWS subjects was the result of pronounced vascular ectasia and proliferations of thin and/or thick-walled vessels and their stroma.¹⁷ However, the detailed molecular mechanism(s) underlying hypertrophy and the formation of nodules within PWS lesions remain obscure. Our previous data from limited nodular biopsies have indicated that PI3K and PLC- γ are activated in PWS nodular lesions. Furthermore, the *Pi3kca* mutation (p.G1049N) has been identified in nodular lesions from one PWS subject,¹² which may contribute to the activation of PI3K. Moreover, *Pi3kca* mutations have been identified in many other vascular malformations, such as venous and lymphatic malformations.^{18,19} This evidence leads us to hypothesize that the PI3K and PLC- γ pathways play important roles in PWS nodular development. In this study, we performed

a full investigation of the activation profiles of PI3K, PKC α , PLC- γ , and PDPK1 in PWS nodules. We found that all of them have strong activation in PWS ECs in ectatic thin or thick-walled blood vessels and in proliferated pericytes and fibroblasts, which directly supports our hypothesis. This study, together with our previous reports,^{10,20} is the first time that the molecular pathological signaling pathways underlying PWS hypertrophy and nodularity have been revealed.

Nodules are estimated to occur in 44% of untreated patients with an average age onset of 22 years²¹; other reports show that the nodular percentage in mixed subjects with treated or untreated PWS is approximately 10% with a mean onset in the 20–39-year age group.^{22,23} These variations are probably due to early laser intervention, which can significantly delay the onset of PWS nodularity. Hypertrophy and nodularity respond poorly to most vascular lasers.^{24–28} Thus, new treatments are required for managing this challenging clinical problem. In our previous investigations, we have proposed that a better PWS therapeutic outcome might be achieved with PDL combined with the administration of antiangiogenesis agents.^{29–32} In this study, we have confirmed that PKC α , PI3K, PLC- γ , and PDPK1 are strongly activated in PWS nodular lesions, suggesting their pivotal roles in nodular formation. Therefore, laser combined with administration of inhibitors of these kinases, and their associated pathways, may be a potentially novel therapeutic strategy for nodular PWS subjects.

In summary, we have shown a progressive activation of PKC α , PDPK1, and PLC- γ and increases in the expression of

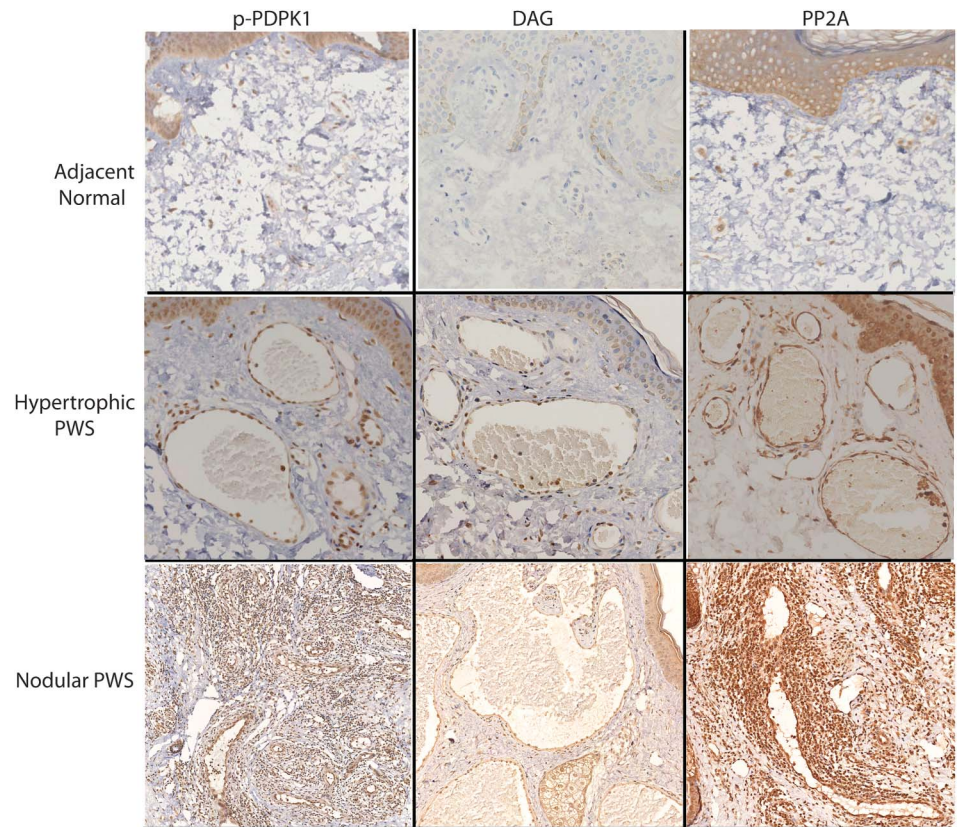


FIGURE 3. Activation of PDPK1 and expressions of DAG and PP2A in the blood vessels from different types of PWS lesions.

PP2A and DAG in PWS hypertrophic and nodular lesions, which are positively correlated with the pathological progression of this disease. Our data have confirmed that both PKC α and PI3K signaling pathways play very critical roles in the

development of PWS hypertrophy and nodularity, suggesting potential applications of antagonists to these kinases as a possible treatment strategy for hypertrophic and nodular PWS.

REFERENCES

1. Mulliken JB, Young AR. *Vascular Birthmarks—Hemangiomas and Malformations*. Philadelphia, PA: W.B. Saunders Co.; 1988.
2. Jacobs AH, Walton RG. The incidence of birthmarks in the neonate. *Pediatrics*. 1976;58:218–222.
3. Pratt AG. Birthmarks in infants. *Arch Dermatol Syphilol*. 1953;67:302–305.
4. Heller A, Rafman S, Zvagulis I, et al. Birth-defects and psychosocial adjustment. *Am J Dis Child*. 1985;139:257–263.
5. Malm M, Carlberg M. Port-wine stain—a surgical and psychological problem. *Ann Plast Surg*. 1988;20:512–516.
6. Kalick SM. Toward an interdisciplinary psychology of appearances. *Psychiatry*. 1978;41:243–253.
7. Lever WF, Schaumburg-Lever G. *Histopathology of the skin*. 7th ed. Philadelphia, PA: J.B. Lippincott Co; 1990.
8. Geronemus RG, Ashinoff R. The medical necessity of evaluation and treatment of port-wine stains. *J Dermatol Surg Oncol*. 1991;17:76–79.
9. Sanchez-Carpintero I, Mihm MC, Mizeracki A, et al. Epithelial and mesenchymal hamartomatous changes in a mature port-wine stain: morphologic evidence for a multiple germ layer field defect. *J Am Acad Dermatol*. 2004;50:608–612.
10. Tan W, Chernova M, Gao L, et al. Sustained activation of c-Jun N-terminal and extracellular signal-regulated kinases in port-wine stain blood vessels. *J Am Acad Dermatol*. 2014;71:964–968.
11. Populo H, Vinagre J, Lopes JM, et al. Analysis of GNAQ mutations, proliferation and MAPK pathway activation in uveal melanomas. *Br J Ophthalmol*. 2011;95:715–719.
12. Lian CG, Sholl LM, Zakka LR, et al. Novel genetic mutations in a sporadic port-wine stain. *JAMA Dermatol*. 2014;150:1336–1340.

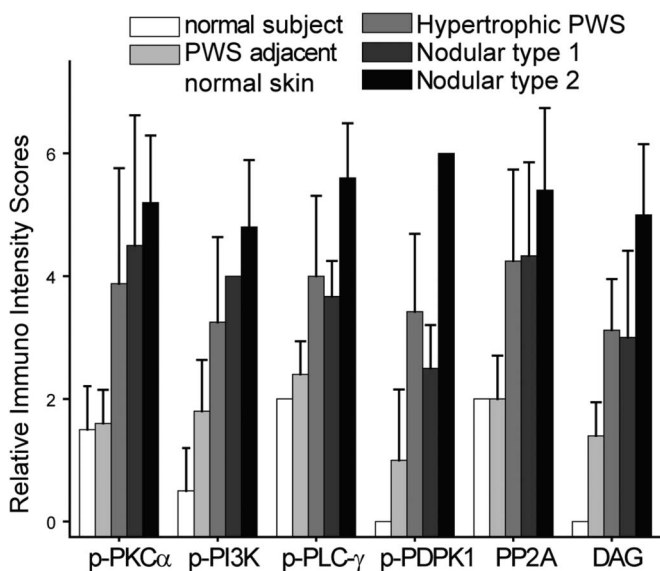


FIGURE 4. Relative IR intensity scores of p-PI3K, p-PKC α , p-PLC- γ , p-PDPK1, DAG, and PP2A in the blood vessels from different types of PWS lesions.

13. Shirley MD, Tang H, Gallione CJ, et al. Sturge-Weber syndrome and port-wine stains caused by somatic mutation in GNAQ. *N Engl J Med*. 2013;368:1971–1979.
14. Luks VL, Kamitaki N, Vivero MP, et al. Lymphatic and other vascular malformative/overgrowth disorders are caused by somatic mutations in PIK3CA. *J Pediatr*. 2015;166:1048–1054. e1–5.
15. Couto JA, Huang L, Vivero MP, et al. Endothelial cells from capillary malformations are enriched for somatic GNAQ mutations. *Plast Reconstr Surg*. 2016;137:77e–82e.
16. Tan W, Nadora DM, Gao L, et al. The somatic GNAQ mutation (R183Q) is primarily located in port wine stain blood vessels. *J Am Acad Dermatol*. 2016;74:380–383.
17. Finley JL, Noe JM, Arndt KA, et al. Port-wine stains. Morphologic variations and developmental lesions. *Arch Dermatol*. 1984;120:1453–1455.
18. Boscolo E, Coma S, Luks VL, et al. AKT hyper-phosphorylation associated with PI3K mutations in lymphatic endothelial cells from a patient with lymphatic malformation. *Angiogenesis*. 2015;18:151–162.
19. Limaye N, Kangas J, Mendola A, et al. Somatic activating PIK3CA mutations cause venous malformation. *Am J Hum Genet*. 2015;97:914–921.
20. Tan W, Zakka LR, Gao L, et al. Pathological alterations involve the entire skin physiological Milieu in infantile and early childhood port wine stain. *Br J Dermatol*. 2016. DOI: 10.1111/bjd.15068.
21. Lee JW, Chung HY, Cerrati EW, et al. The natural history of soft tissue hypertrophy, bony hypertrophy, and nodule formation in patients with untreated head and neck capillary malformations. *Dermatol Surg*. 2015;41:1241–1245.
22. Mills CM, Lanigan SW, Hughes J, et al. Demographic study of port wine stain patients attending a laser clinic: family history, prevalence of naevus anaemicus and results of prior treatment. *Clin Exp Dermatol*. 1997;22:166–168.
23. Klapman MH, Yao JF. Thickening and nodules in port-wine stains. *J Am Acad Dermatol*. 2001;44:300–302.
24. Izikson L, Nelson JS, Anderson RR. Treatment of hypertrophic and resistant port wine stains with a 755 nm laser: a case series of 20 patients. *Lasers Surg Med*. 2009;41:427–432.
25. Kono T, Frederick Groff W, Chan HH, et al. Long-pulsed neodymium: yttrium-aluminum-garnet laser treatment for hypertrophic port-wine stains on the lips. *J Cosmet Laser Ther*. 2009;11:11–13.
26. Chen D, Hu XJ, Lin XX, et al. Nodules arising within port-wine stains: a clinicopathologic study of 31 cases. *Am J Dermatopathol*. 2011;33:144–151.
27. del Pozo J, Fonseca E. Port-wine stain nodules in the adult: report of 20 cases treated by CO2 laser vaporization. *Dermatol Surg*. 2001;27:699–702.
28. Tierney EP, Hanke CW. Treatment of nodules associated with port wine stains with CO2 laser: case series and review of the literature. *J Drugs Dermatol*. 2009;8:157–161.
29. Gao L, Phan S, Nadora DM, et al. Topical rapamycin systematically suppresses the early stages of pulsed dye laser-induced angiogenesis pathways. *Lasers Surg Med*. 2014;46:679–688.
30. Nelson JS, Jia W, Phung TL, et al. Observations on enhanced port wine stain blanching induced by combined pulsed dye laser and rapamycin administration. *Lasers Surg Med*. 2011;43:939–942.
31. Tan W, Jia W, Sun V, et al. Topical rapamycin suppresses the angiogenesis pathways induced by pulsed dye laser: molecular mechanisms of inhibition of regeneration and revascularization of photocoagulated cutaneous blood vessels. *Lasers Surg Med*. 2012;44:796–804.
32. Gao L, Nadora DM, Phan S, et al. Topical axitinib suppresses angiogenesis pathways induced by pulsed dye laser. *Br J Dermatol*. 2015;172:669–676.